Byrne, P, Mayes, WM, James, AL, Comber, S, Biles, E, Riley, AL, Verplanck, PL and Bradley, L

Spatially resolved source apportionment of per- and polyfluoroalkyl substances (PFAS) within a post-industrial river catchment

Science of the Total Environment 1001 (2025) 180502

Contents lists available at ScienceDirect

Science of the Total Environment

journal homepage: www.elsevier.com/locate/scitotenv

Spatially resolved source apportionment of per- and polyfluoroalkyl substances (PFAS) within a post-industrial river catchment

Patrick Byrne [a,*], William M. Mayes [b], Alun L. James [c], Sean Comber [d], Emma Biles [a], Alex L. Riley [b], Philip L. Verplanck [e], Lee Bradley [a]

[a] School of Biological and Environmental Sciences, Liverpool John Moores University, Liverpool, L3 3AF, United Kingdom
[b] School of Environmental and Life Sciences, University of Hull, Hull, HU6 7RX, United Kingdom
[c] Environment Agency, Bristol, BS1 5AH, United Kingdom
[d] School of Geography, Earth and Environmental Sciences, University of Plymouth, Drakes Circus, Plymouth, PL4 8AA, United Kingdom
[e] U.S. Geological Survey, Denver Federal Center, P.O. Box 25046, Mail Stop 973, Denver, CO, 80225, United States

HIGHLIGHTS

- Load-based methods better define PFAS sources than concentration data alone.
- Largest PFAS river loads observed in sub-catchments with lower concentrations.
- PFAS yield was highest in headwater catchments with confirmed industrial sources.
- Gadolinium tracing linked PFAS to industry discharges at 62 % of sample sites.
- Spatial load analysis is vital for identifying and prioritising PFAS remediation.

GRAPHICAL ABSTRACT

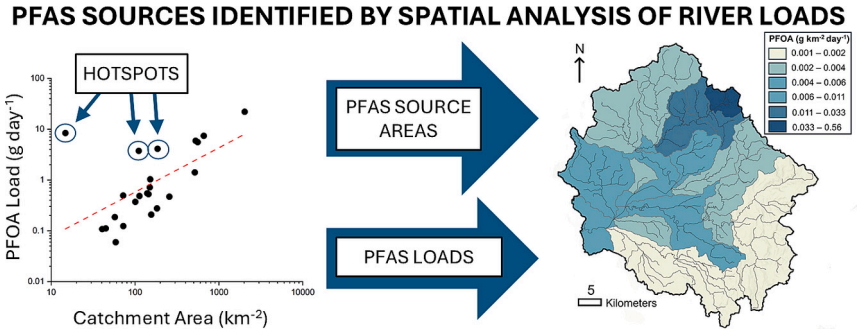

ARTICLE INFO

Keywords:
Forever chemicals
Watershed
Loads
Flux
Synoptic sampling
Gadolinium
Land use

ABSTRACT

Source apportionment of *per-* and polyfluoroalkyl substances (PFAS) in rivers is typically based on water concentrations, which cannot quantify PFAS loads or define geographical source areas. This study applied a river catchment-scale approach to identify PFAS source zones and assess the relative importance of industrial PFAS sources in the River Mersey, UK – a post-industrial, densely populated catchment with diverse PFAS sources. Synoptic sampling and PFAS river load analysis identified key sub-catchments and river stretches contributing the majority of PFAS. Notably, the highest PFAS concentrations did not always correspond to the greatest loads. Most PFOS (64 %), PFOA (49 %), 6:2FTS (46 %) and PFHxS (56 %) were exported from the Upper Mersey sub-catchment, despite higher concentrations in northern sub-catchments, emphasising the importance of load-based monitoring. Mass balance analysis of loads highlighted substantial inputs from specific river stretches, notably the Lower Irwell (Bolton to Manchester City Centre), River Tame (Marple Bridge to Stockport), and Upper Mersey (Stockport to Urmston). While PFAS loads generally scaled with catchment area, yield (load per unit area) analysis identified disproportionately high exports from small headwater catchments, notably the upper River Roch (PFOA, PFHpA and PFHxA) and Glaze Brook (PFBS). Industrial sources in these sub-catchments (a waste management facility and landfills, respectively) were confirmed using gadolinium anomaly analysis and

* Corresponding author.
E-mail address: p.a.byrne@ljmu.ac.uk (P. Byrne).

https://doi.org/10.1016/j.scitotenv.2025.180502
Received 13 June 2025; Received in revised form 11 August 2025; Accepted 11 September 2025
Available online 19 September 2025

consented discharge records. More widely, gadolinium data suggested industrial discharges may contribute to PFAS occurrence at 62 % of our sample sites throughout the catchment. These findings demonstrate that spatial analysis of PFAS loads, rather than concentrations alone, is critical for identifying PFAS source areas. We present a scalable monitoring framework for PFAS source apportionment applied at the river catchment-scale that can be used by environmental managers to target and prioritise PFAS source areas for detailed monitoring and remediation.

1. Introduction

Per- and polyfluoroalkyl substances (PFAS) are a class of more than 10,000 compounds containing at least one fully fluorinated methyl or methylene carbon atom (European Chemicals Agency, 2023). PFAS are extremely resistant to chemical and thermal degradation and utilised in thousands of consumer products from food packaging to personal care products and in almost all industrial and manufacturing processes (notably fire-fighting foams) since the 1950s (Kurwadkar et al., 2022). Due to their extreme persistence, PFAS have been detected in environments and wildlife worldwide (Cousins et al., 2022; Evich et al., 2022; Garnett et al., 2021). PFAS have been detected in human serum (Ho et al., 2022), and the most studied compounds are linked to a range of negative health outcomes in humans (Garg et al., 2020; Obsekov et al., 2023; Pelch et al., 2022).

For several decades, a major strand of PFAS research has focussed on occurrence and concentrations in rivers given their importance as food and drinking water sources and because rivers are important vectors for the transport of PFAS from primary sources on land to the oceans (Byrne et al., 2024; Cai et al., 2025). Recent syntheses of global surface water (including rivers) concentrations indicate PFAS are near ubiquitous in rivers (Ackerman Grunfeld et al., 2024; Calore et al., 2023; Kurwadkar et al., 2022). Global median concentrations of the most studied individual compounds vary from approximately 3 to 20 ng L^{-1}, with perfluorooctanoic acid (PFOA) and perfluorobutanoic acid (PFBA) typically occurring at the highest concentrations (Byrne et al., 2025; Calore et al., 2023). Surface water concentrations in China are elevated compared to western countries with rivers receiving most (57.6 %) of the PFAS environmental emissions in China (Calore et al., 2023). Benchmarking global surface water PFAS concentrations ($n = 9479$) against threshold regulatory limits, Ackerman Grunfeld et al. (2024) estimated that up to 84 % of global surface waters fail to meet the Canadian sum of all PFAS criteria (sum total of 25 specific PFAS less than 30 ng L^{-1}) (Health Canada, 2023) and up to 54 % fail to meet the EU sum of all PFAS criteria (sum total of 20 specific PFAS less than 500 ng L^{-1}) (EU, 2020).

The next challenge for PFAS river science is source apportionment to inform catchment or site-specific management and remediation. The potential sources of PFAS in river catchments are well documented and can include effluent from primary sources such as PFAS manufacturers and industry (Megson et al., 2024; Petre et al., 2022), and secondary sources such as effluents from wastewater treatment works (WwTWs) (Cookson and Detwiler, 2022), leachates and runoff from landfills (Zhang et al., 2023), agricultural land (Biswas et al., 2025), airports and military bases (Ruyle et al., 2023). A common approach to source apportionment is to relate PFAS river water concentrations to land use characteristics and nearby potential sources through multi-variate analyses (Breitmeyer et al., 2023; Yao et al., 2014; Zhang et al., 2016a). The fingerprinting approach uses PFAS chemical signatures to constrain PFAS detected in river water to certain industrial activities or processes (Charbonnet et al., 2021). If the PFAS signature is unique and can be mapped to a specific industrial facility or historical process (a primary source), the fingerprinting approach can be used to identify sources (Joseph et al., 2023). However, the fingerprinting approach requires complex multi-variate analyses and expert knowledge of PFAS chemistry and potentially has limited utility for secondary sources like WwTW and landfills which contain many PFAS compounds from diverse sources and time periods. Furthermore, these approaches cannot isolate the geographical contributing areas of PFAS input at the river catchment-scale, nor can they establish how much PFAS (the PFAS load) enters a river from these areas. For persistent chemicals like PFAS that are considered chronically toxic, the total amount present in the environment is arguably more important than the concentration. As these substances do not break down easily and can accumulate over time, a high load means greater long-term exposure risks for ecosystems and humans, especially through bioaccumulation and food chains. Loads also better reflect the potential for PFAS to disperse and persist across regions, making it a more meaningful measure for environmental impact and regulatory decisions. Furthermore, analysis of spatial patterns in PFAS loads allows one to quantify and rank sources, so that the largest sources (in terms of PFAS mass) can be the subject to remedial interventions.

Mass balance analysis of river PFAS loads can help catchment managers constrain PFAS geographical source areas and prioritise interventions based on the mass of PFAS entering rivers. Temporal analysis and modelling of observed PFAS river loads upstream and downstream of a PFAS manufacturing plant in North Carolina, USA, established the point source PFAS loading from the facility and the temporal trend in PFAS export from the catchment (Petre et al., 2022). Our work, in the River Mersey catchment in the United Kingdom (UK), established the first temporally-robust estimates of PFAS export for a major European river system (Byrne et al., 2024). Furthermore, analysis of PFAS loads at the river catchment outlet and from WwTWs demonstrated quantitatively that perfluorooctane sulfonic acid (PFOS) from WwTWs accounted for only 50 % of the total PFOS river export, suggesting non-WwTW sources are significant in post-industrial and heavily urbanised river catchments. Although the studies of Byrne et al. (2024) and Petre et al. (2022) successfully quantified the loads associated with major and known point sources (industry and WwTWs), the load contribution from unknown point and non-point sources is difficult to establish. A potential approach to establish PFAS source areas and loads across mixed-source river catchments is analysis of spatial patterns in PFAS loads collected under steady river flow conditions. This synoptic sampling approach has been widely used to locate and quantify sources of trace metal(loids) in mineralised and mining-impacted river catchments for remediation interventions (Byrne et al., 2020; Mayes et al., 2008; Runkel et al., 2023). A similar approach, using time of travel sampling, was used to establish PFAS loads and sources linearly along the Neshaminy Creek, Pennsylvania, USA (Woodward et al., 2024). As far as we are aware, no published studies have attempted synoptic sampling across a large (>2000 km^{-2}) and highly urbanised river catchment to investigate PFAS sources and loads.

In this study, we present a river catchment-scale investigation of PFAS concentrations and loads in an urbanised, post-industrial and hydrologically complex river system (the River Mersey, UK) to identify PFAS geographical source areas and to establish the relative importance of industrial sources for PFAS transport through rivers. Our specific objectives were to: i) establish spatial patterns of PFAS concentrations across a heavily urbanised river basin; ii) constrain the geographical source areas of PFAS within the river basin, and iii) estimate the relative importance of industrial sources in controlling PFAS river water concentrations.

2. Methodology

2.1. Study site

The wider Manchester conurbation is the second most populous urban area (2.8 million people) in the UK. The region is located in the River Mersey catchment, comprising the Upper River Mersey, River Irwell, River Irk, River Medlock, River Bollin, Glaze Brook and Sinderland Brook sub-catchments (total catchment area = 2030 km^2) (Fig. S1). The drainage system rises in the Pennine moorland to the north and east of the river catchment, and in the Cheshire Plain lowland to the south. The drainage system is heavily modified and urbanised (42 %), containing a mixture of land uses and activities typical of many post-industrial river catchments where high PFAS concentrations have been recorded (Evich et al., 2022). A notable modification of the drainage system is the Manchester Ship Canal (MSC), a navigable 58 km long channel connecting central Manchester to the River Mersey Estuary and the Irish Sea. Several major tributaries of the Mersey flow into the MSC as well as effluents from numerous WwTWs – some of these WwTWs receive water from outside of the catchment. Fig. 1 highlights numerous potential PFAS sources (1950s to present) that exist in the catchment, including effluents from WwTWs, landfills, industry (metal plating and manufacture of chemicals, textiles, and electronics), agriculture and airports, though concentration and loading data are only known for WwTWs (Byrne et al., 2024).

2.2. River water sampling

River water samples for PFAS analysis were collected at 63 locations across the Mersey catchment (Fig. 2) under moderately low (Q70) to moderately high (Q20) flow conditions (measured at the catchment outlet at sample site M20-H19) (National River Flow Archive (NRFA), 2024) between 14th and 30th August 2023 (Fig. S2). Sample sites were selected to represent all major and minor tributary rivers and, where possible, several samples were collected from the source of a tributary to its downstream confluence to capture linear changes in PFAS loads and

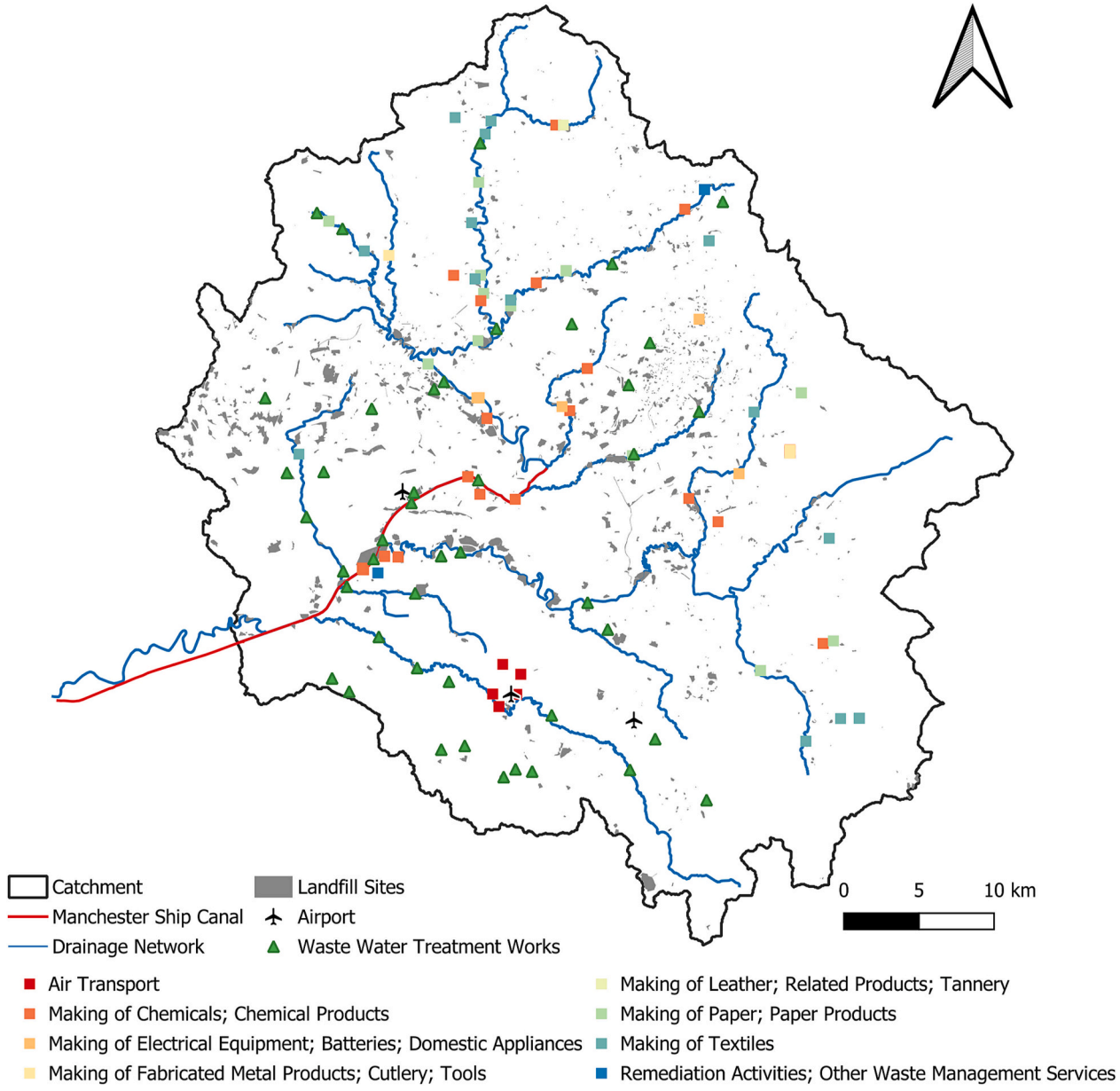

Fig. 1. River Mersey catchment showing the locations of potential PFAS sources. Source data were obtained from the Environment Agency Consented Discharge dataset (Environment Agency, 2025).

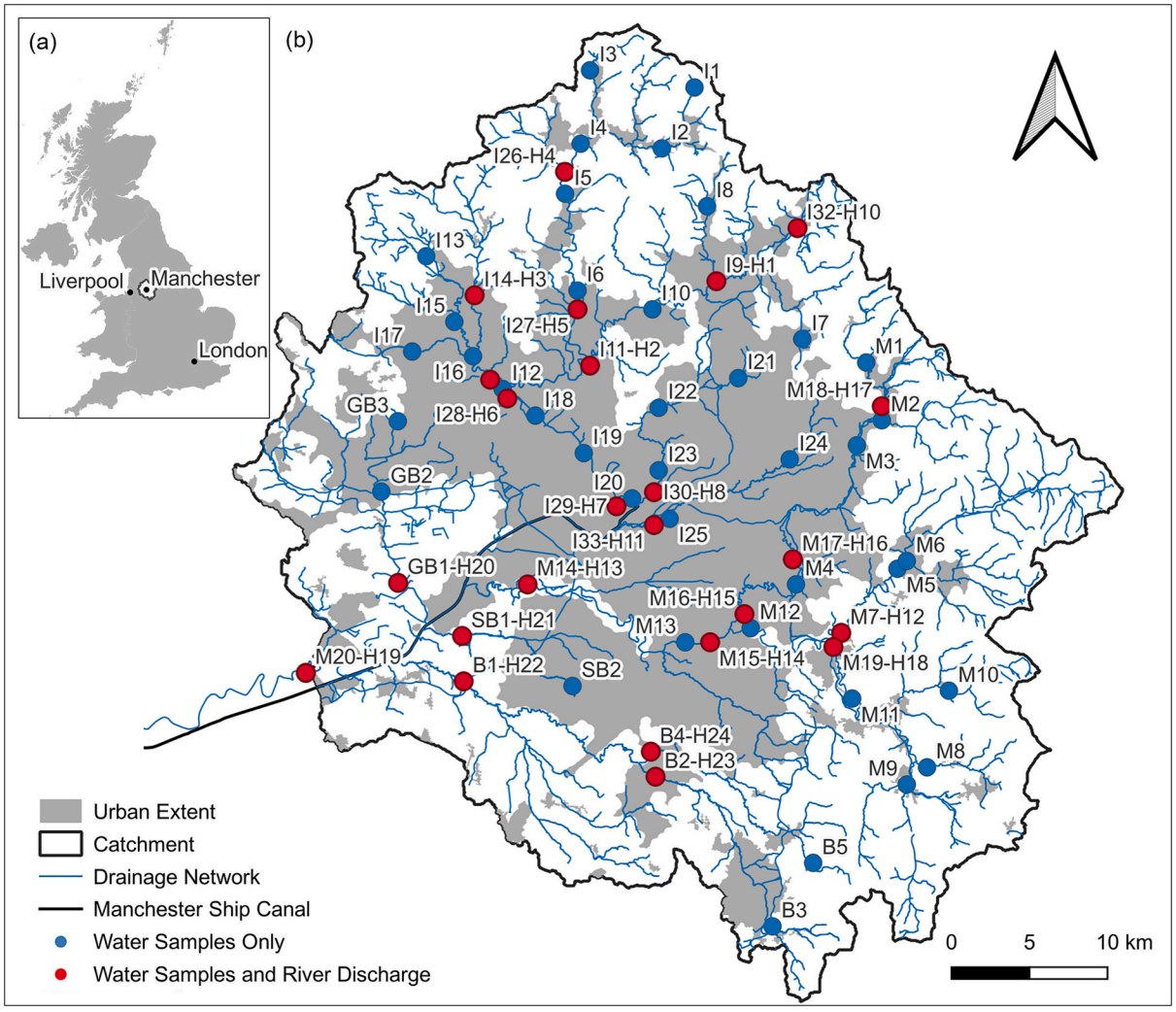

Fig. 2. The River Mersey catchment showing the drainage network, urban extent (grey coverage) and the locations and sample IDs of 63 sample locations from August 2023. Blue circles show samples sites where water only samples were collected ($n = 40$) and red circles show sites where water samples and river discharge measurements were taken ($n = 23$). Source of drainage network data is EDINA Digimap Ordnance Survey Service (2025).

concentrations. Unfiltered water samples were collected from below the water surface and in the centroid of flow using a 2 L high-density polyethylene (HDPE) bottle. Samples were then decanted into two 50 mL HDPE tubes for laboratory analysis of 17 PFAS [9 perfluoroalkylcarboxyclic acids (PFCAs), 6 perfluoroalkylsulfonates (PFSAs), perfluorooctanesulfonamide (PFOSA), and 6:2 fluorotelomer sulfonate (6:2FTS)] by LC-MS/MS (Table S1). The PFAS analysis suite reflects the most commonly detected compounds in river water worldwide (Calore et al., 2023) and by the Environment Agency in England (Environment Agency, 2021), however we acknowledge that emerging evidence suggests a greater number of compounds may be present in river water (Joerss et al., 2022). Further information on PFAS sampling and analytical procedures can be found in the Supplementary Information.

2.3. Load estimation

Synoptic water sampling at 23 river flow gauges was conducted across the Mersey Basin on the 22nd and 23rd of August 2023 (Fig. 2 – red circles). Sampling was conducted under steady river flow conditions (Fig. S2) so that spatial patterns of PFAS loads could be used to identify geographical source areas and sinks of PFAS within the river system. The daily loads (g day^{-1}) of individual PFAS compounds at each of the 23 gauged sample sites were calculated as the product of the measured water sample concentrations (ng L^{-1}) and the observed river discharge (L s^{-1}) extrapolated to a daily load. River discharge data (within ±15 min of water sample collection) at the time of PFAS sampling were obtained from the National River Flow Archive (National River Flow Archive (NRFA), 2024). PFAS loads were also estimated for the MSC at Latchford Locks using historical data (1997 to 2002) from the Environment Agency of England gauge at the Latchford Locks (Supplementary Information). PFAS yield was also calculated for sites with combined concentration and flow data by dividing estimated load by catchment area (National River Flow Archive (NRFA), 2024).

2.4. Gadolinium anomalies

A stable gadolinium (Gd) compound is used as a paramagnetic contrasting agent in magnetic resonance imaging (MRI) and persists through urban WwTWs and the receiving river (Lawrence, 2010; Verplanck et al., 2010). When plotting rare earth element (REE) concentration data, urban WwTW effluent displays a positive Gd enrichment called a Gd anomaly (Bau and Dulski, 1996; Verplanck et al., 2005). We utilise Gd anomalies to evaluate the potential spatial relationship between river water PFAS concentrations with both a WwTW and non-WwTW (industrial) signal. Water samples for REE analysis were collected at the same location and time as the PFAS samples. The samples were filtered with a 0.22 μm pore-size filter membrane and acidified

with concentrated HNO_3 to a pH of <2. REE concentrations were determined by inductively coupled plasma-mass spectrometry (ICP-MS) using an Agilent 7900 instrument. Samples were determined in triplicate using a direct calibration curve quantification technique with 103Rh used as an internal standard.

The size of the gadolinium anomaly can be quantified as the ratio of measured Gd to the expected Gd (Gd*), interpolated from its neighbouring REEs, Samarium (Sm) and Dysprosium (Dy), after normalisation using a reference material (the North American Shale Composite). Samarium and Dy were selected for interpolation as they do not have interfering isotopes or multiple redox states that could bias the calculated baseline concentration. To assess whether samples were affected by anthropogenic Gd inputs, we also calculated the proportion of Gd relative to the total REE content (Gd% = [Gd] / Σ[REE] x 100). Samples where Gd contributed more than 15 % of total REEs generally exhibited a clear positive anomaly (Gd/Gd* > 3), consistent with wastewater-derived inputs. Therefore, we used >15 % Gd as a threshold to distinguish samples impacted by WwTW effluent from those showing only natural variability (Fig. S3).

3. Results and discussion

3.1. PFAS concentrations and spatial patterns

Eleven of the seventeen targeted PFAS were detected across the River Mersey catchment with detection frequencies between 2 % (perfluorodecanoic acid, PFDA) and 97 % (PFOA) (Table S2). Median concentrations ranged from 1.31 ng L^{-1} (perfluorohexane sulfonic acid, PFHxS) to 5.31 ng L^{-1} (PFOS) (Fig. 3), which is similar to other studies of urban river catchments (Breitmeyer et al., 2023; Cookson and Detwiler, 2022; Zushi et al., 2011) and global surface water data (Ackerman Grunfeld et al., 2024; Calore et al., 2023). Peak concentrations and the greatest range in concentrations were for PFOA (270 ng L^{-1}; range = 269.27 ng L^{-1}), PFBS (110 ng L^{-1}; range = 108.83 ng L^{-1}) and PFHxA (44.9 ng L^{-1}; range = 43.72 ng L^{-1}). Comparing the measured PFAS concentrations in river water to threshold regulatory concentrations, we estimate that all of our samples would meet the EU sum of all PFAS criteria (sum total less than 500 ng L^{-1}) (EU, 2020), however 35 % of our samples would fail to meet the stricter Canadian sum of all PFAS criteria (sum total less than 30 ng L^{-1}) (Health Canada, 2023). Although River Mersey water is not used as drinking water, drinking water standards provide a valuable benchmark. Furthermore, it is highly likely that our targeted analytical approach (17 compounds) underestimates the total PFAS concentrations in our samples, as found in studies using non-targeted or total PFAS analytical approaches (Ateia et al., 2023; Megson et al., 2024).

Fig. 4 illustrates the concentrations of PFOS, PFOA and the sum of nine most frequently detected PFAS spatially across the River Mersey catchment. PFOS concentrations (Fig. 4a) generally increased with distance downstream in sub-catchments. As a result, elevated PFOS concentrations occurred where the rivers Irwell, Irk and Medlock converge in Manchester city centre. The highest PFOS concentration occurred in the Upper Mersey (M14-H13; 25.6 ng L^{-1}) before it discharges into the MSC. Increasing concentrations downstream in urban catchments has been reported elsewhere and related to increases in the percentage of urban area upstream of sampling points (Breitmeyer et al., 2023; Zhang et al., 2016a; Zushi et al., 2011). In the River Mersey catchment, this urbanisation signal is likely driven by the accumulation of point source discharges from industry and WwTWs (Fig. 1). Historical landfills are also widespread in the lower catchment and typically located close to the river channel (e.g. in the lower part of the Upper Mersey sub-catchment) where non-point and point discharges of leachate probably contribute to increases in PFAS concentrations in rivers (Neill and Megson, 2024). The spatial pattern in PFOA (Fig. 4b), PFBS and PFBA concentrations (Fig. S4) was different from PFOS with notably higher concentrations in the north of the Mersey catchment in the rivers Irk,

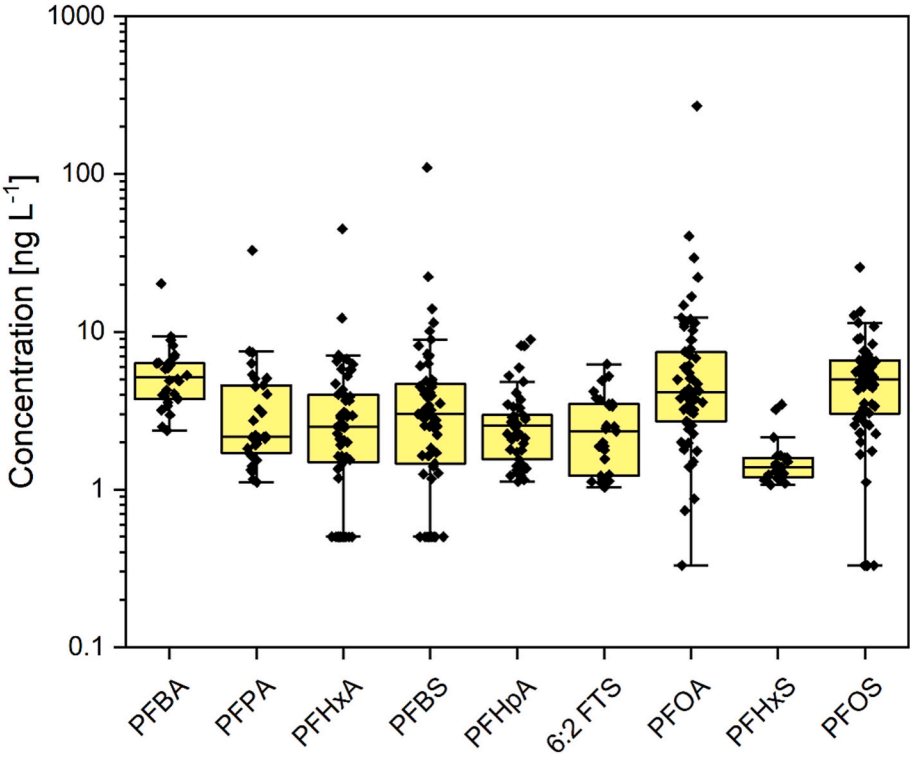

Fig. 3. Nine PFAS compounds detected in 63 river water samples collected across the River Mersey Basin in August 2023. Perfluorodecanoic acid (PFDA) and perfluorononanoic acid (PFNA) are excluded from the figure as their detection frequency was less than 5 %. The yellow box represents the interquartile range, and the internal black line is the median value. The upper and lower whiskers represent 1.5 times the interquartile range. Black diamonds represent individual samples, with samples lower or higher than the whiskers defined as outliers.

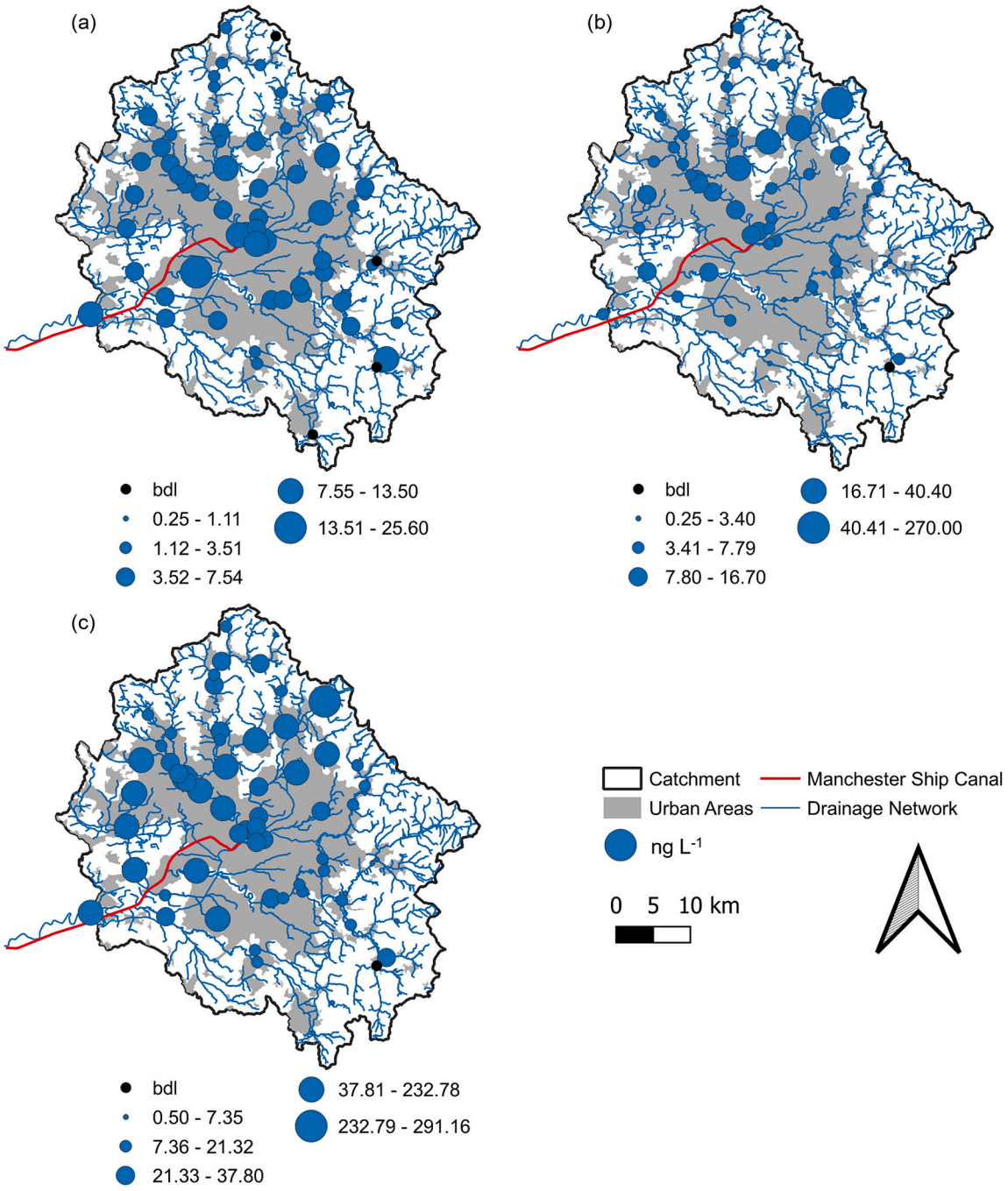

Fig. 4. Proportional circles maps of PFOS (a), PFOA (b) and sum of nine PFAS concentrations (c). bdl = below detection limit.

Irwell and Glaze Brook. This pattern is evident in the sum of nine PFAS concentrations (Fig. 4c) indicating these compounds dominate the PFAS signal. Historically, the rivers Irk and Irwell have been major centres for textile production in riparian areas, as well as containing paper mills, collieries and an associated coal-fired power station (in the lower Irwell); chemical industries producing synthetic dyes and finishing products (Irk), printworks, metal plating, wire and cable manufacturing facilities have been present in the Irk catchment.

Although concentrations generally increased downstream in the catchment, some notable exceptions are evident where elevated concentrations were consistently found in headwater catchments. Elevated PFOS concentrations were detected in Black Brook in the Upper Mersey (M8; 12.7 ng L^{-1}), the River Beal in the Roch catchment (I7; 8.38 ng L^{-1}), and Glaze Brook (GB2; 7.18 ng L^{-1}). The highest PFOA concentrations were recorded in the headwaters of the River Roch (I32-H10; 270 ng L^{-1}) and these elevated concentrations persisted to the confluence with the MSC in central Manchester. The highest PFBS concentration was detected in the headwaters of Glaze Brook (GB3; 110 ng L^{-1}) which also had elevated PFOA (GB3; 11.4 ng L^{-1}) and the highest recorded PFBA concentrations (GB3; 20.2 ng L^{-1}). Elevated concentrations of other compounds were also detected in Glaze Brook (PFPA, PFHxA), the River Beal (PFPA, PFHxA; PFHxS), the River Roch (PFHxA), and Sinderland Brook (PFPA; PFHxA; PFHxS).

The Environment Agency (EA) database of Consented Discharges to Controlled Waters (Environment Agency, 2025) highlights several potential industrial PFAS sources in these catchments which might account for the elevated concentrations – these are mapped in Fig. 1. In the River Roch, elevated PFOA and PFHxA at site I32-H10 occurred downstream

of trade discharges from a waste management facility. Other potential industrial sources along this stretch of river include discharges from chemicals, paper and foam producers, textiles manufacturers and Bury WwTW. The River Beal, which discharges into the River Roch below I32-H10, had elevated concentrations of most detected PFAS at site I7 which may be due to discharge from Crompton Effluent Treatment Works – a permitted landfill. In Glaze Brook, we found elevated concentrations of almost all detected PFAS, in particular in the upper catchment in Carr Brook at site GB3. PFBS in particular is a major component of landfill leachate (Knutsen et al., 2019; Liu et al., 2024), and two permitted landfills (Holcroft Hall Quarry Landfill Site and Risley Landfill) are located in the headwaters of this sub-catchment above site GB3. Elevated PFAS concentrations persist further downstream at site GB1-H20 which is downstream of high PFAS discharges from Irlam, Tyldesley and Leigh WwTWs.

3.2. PFAS loads and geographical source areas

Table 1 summarises the PFAS loads measured at samples sites ($n = 7$) located at the outlets of the seven major sub-catchments. The largest PFOS (62 %; 12.85 g day^{-1}), PFOA (49 %; 7.38 g day^{-1}), 6:2FTS (46 %; 3.12 g day^{-1}), and PFHxS (56 %; 1.73 g day^{-1}) loads were sourced from the Upper Mersey sub-catchment despite the general pattern of higher concentrations in the north of the Mersey catchment. This might be explained by the larger catchment area of the Upper Mersey (37 %) compared with the Irwell (30 %). PFHxA loads were highest in the Irwell (31 %; 4.95 g day^{-1}) and PFHpA loads were similar in both sub-catchments (Upper Mersey = 31 %; 1.44 g day^{-1} and Irwell = 32 %; 1.45 g day^{-1}). Of note, Glaze Brook had the highest PFBS load (39 %; 2.58 g day^{-1}) and the third largest PFOA (7 %; 1.03 g day^{-1}), PFHxA (22 %; 1.41 g day^{-1}) and PFHpA loads (15 %; 0.69 g day^{-1}) despite only representing 9 % of the total area of the seven sub-catchments. The River Bollin contributed the third largest PFOS, 6:2FTS and PFHxS loads and represents 12 % of the area of the sub-catchments.

Analysis of the spatial pattern of PFAS loads across all twenty-three sample sites allows quantification of changes in loads change from upstream to downstream and the identification of source areas. Fig. 5 illustrates PFOS, PFOA and the sum of seven PFAS (PFOS, PFOA, PFBS, PFHxA, PFHxS, 6:2FTS and PFHpA) loads throughout the Mersey catchment as Sankey plots. In these plots, the thickness of the line is proportional to the PFAS load, and the grey lines represent stretches of river where there is an increase in load. For example, the rivers Roch, Croal and Upper Irwell flow into the Lower Irwell. The PFOS load contribution from the River Roch (I11-H2; 2.5 g day^{-1}) is greater than the River Croal (I31-H9; 0.61 g day^{-1}) and the Upper Irwell (I27-H5; 0.44 g day^{-1}) (Table S3). The PFOA load contribution from the River Roch is also higher (4.1 g day^{-1}) than the Croal (0.53 g day^{-1}) and the Upper Irwell (0.54 g day^{-1}). For both PFOS and PFOA, the total load contribution from the three rivers is less than the load measured farther downstream in the Lower Irwell such that 28 % of PFOS (1.4 g day^{-1}) and 6 % of PFOA (0.36 g day^{-1}) in the Lower Irwell is unaccounted for (Table S4), represented as 'X2' in Fig. 5a and b. This additional load in the Lower Irwell could originate as effluents from landfills, WwTWs, electrical / battery, leather or paper manufacturers located along this stretch of river (Fig. 1). A large increase in load also occurs for both PFOS (11.7 g day^{-1}; 91 %) and PFOA (6.7 g day^{-1}; 90 %) between the River Tame (M16-H15) and the Upper Mersey (M14-H13), represented as 'X3' in Fig. 5a and b, in an area where several WwTWs, landfills and chemicals manufacturers discharge to the river. For all PFAS compounds, there is a large unaccounted-for increase in loads in the Manchester Ship Canal (MSC1), represented as 'X4' in Fig. 5. All seven major sub-catchments discharge into the canal, however, the increase in load measured at the outlet of the sub-catchments and the load estimated for the MSC ranges from 80 % for PFBS to 7 % for PFOS (Table S4). Several WwTWs discharge directly to the MSC (Fig. 1). Only PFOS and PFOA loading data are available for the WwTWs (Byrne et al., 2024), which might explain why these compounds have the lowest percent difference. The discrepancy between loads measured in the sub-catchments and in the MSC could result from error in the MSC PFAS loads, which are estimated rather than observed (Supplementary Information). There may also be unaccounted for sources to the MSC or biological transformation of PFAS precursors within the canal sediments which in WwTWs sometimes increases effluent loads (Moneta et al., 2023; Thompson et al., 2022). Although the general pattern observed was an increase in loads between sample points, a large decrease in PFBS load (89 %) occurred between the Goyt (M19-H18) and the Tame (M16-H15), represented as 'S1' in Fig. S5b. As PFBS is a terminal degradation product, sorption to sediments rather than transformation probably explains the decrease in load in this stretch of river.

Fig. 6 illustrates PFAS load data against catchment area (UK Centre for Ecology and Hydrology, 2025) for the twenty-three load sample sites. In general, there are weak to moderately strong and highly significant ($p < 0.001$ for all compounds except PFOA where $p < 0.004$) correlations between load and catchment area, which suggests PFAS river load scales with catchment area in highly urbanised river catchments. Positive residuals (data above the predicted model line) can be used to highlight catchments with disproportionately large loading. Elevated loads are particularly evident in the River Roch (I9-H1; I32-H10; I11-H2), River Irk (I30-H8) and Glaze Brook (GB1-H20). Of note, PFOA load (8.4 g day^{-1}) in the upper River Roch (I32-H10) with a catchment area of 14.8 km^2 was of similar magnitude to the total PFOA load (22 g day^{-1}) discharged at the outlet of the River Mersey at Westy (M20-H19) with a catchment area of 2030 km^2. We can highlight catchments with disproportionately high loads by calculating the PFAS catchment yield. Catchment yield is calculated as the PFAS load divided by the catchment area upstream of the load monitoring point. The yield metric provides a means of comparing loads from different size catchments by quantifying the PFAS load per unit drainage area. Fig. 7 illustrates PFAS yields for selected catchments in the Mersey – the catchment areas are sourced from the UK National River Flow Archive (UK Centre for Ecology and Hydrology, 2025). The catchment draining to I32-H10 on the River Roch had the largest PFOA (0.564 g km^{-2} day^{-1}), PFHpA (0.019 g km^{-2} day^{-1}) and PFHxA (0.013 g km^{-2} day^{-1}) yields. The catchment draining to GB1-H20 on Glaze Brook had the largest PFBS (0.017 g km^{-2} day^{-1}) yield. The River Irwell at I29-H7 had the largest 6:2FTS (0.005 g km^{-2} day^{-1}) yield and the River Mersey at M14-H13 had the largest PFHxS (0.003 g km^{-2} day^{-1}) and PFOS (0.019 g km^{-2} day^{-1}) yields.

Table 1
PFAS loads (g day^{-1}) measured at the outlet of seven major sub-catchments of the River Mersey. The percentage contribution of catchment area and loads are given in parentheses. PFPA and PFBA are excluded as they were detected at less than half of the load measurement sites.

Catchment (% area) Site ID	PFOS	PFOA	PFHxA	PFBS	PFHpA	6:2 FTS	PFHxS
River Bollin (14 %) B1-H22	1.22 (6 %)	0.47 (3 %)	0.81 (13 %)	0.52 (8 %)	0.45 (10 %)	0.66 (10 %)	0.29 (9 %)
Glaze Brook (9 %) GB1-H20	0.75 (4 %)	1.03 (7 %)	1.41 (22 %)	2.58 (39 %)	0.69 (15 %)	0.13 (2 %)	0.14 (4 %)
Sinderland Brook (2 %) SB1-H21	0.13 (1 %)	0.11 (1 %)	0.12 (2 %)	0.09 (1 %)	0.07 (2 %)	0.01 (0.2 %)	0.04 (1 %)
Upper Mersey (37 %) M14-H13	12.85 (62 %)	7.38 (49 %)	1.55 (24 %)	1.11 (17 %)	1.44 (31 %)	3.12 (46 %)	1.73 (56 %)
River Irwell (30 %) I29-H7	4.95 (24 %)	5.53 (36 %)	1.99 (31 %)	2.08 (31 %)	1.45 (32 %)	2.57 (38 %)	0.77 (25 %)
River Medlock (3 %) I33-H11	0.29 (1 %)	0.19 (1 %)	0.07 (1 %)	0.03 (1 %)	0.08 (2 %)	0.03 (0.5 %)	0.04 (1 %)
River Irk (4 %) I30-H8	0.62 (3 %)	0.49 (3 %)	0.48 (7 %)	0.24 (4 %)	0.40 (9 %)	0.20 (3 %)	0.10 (3 %)

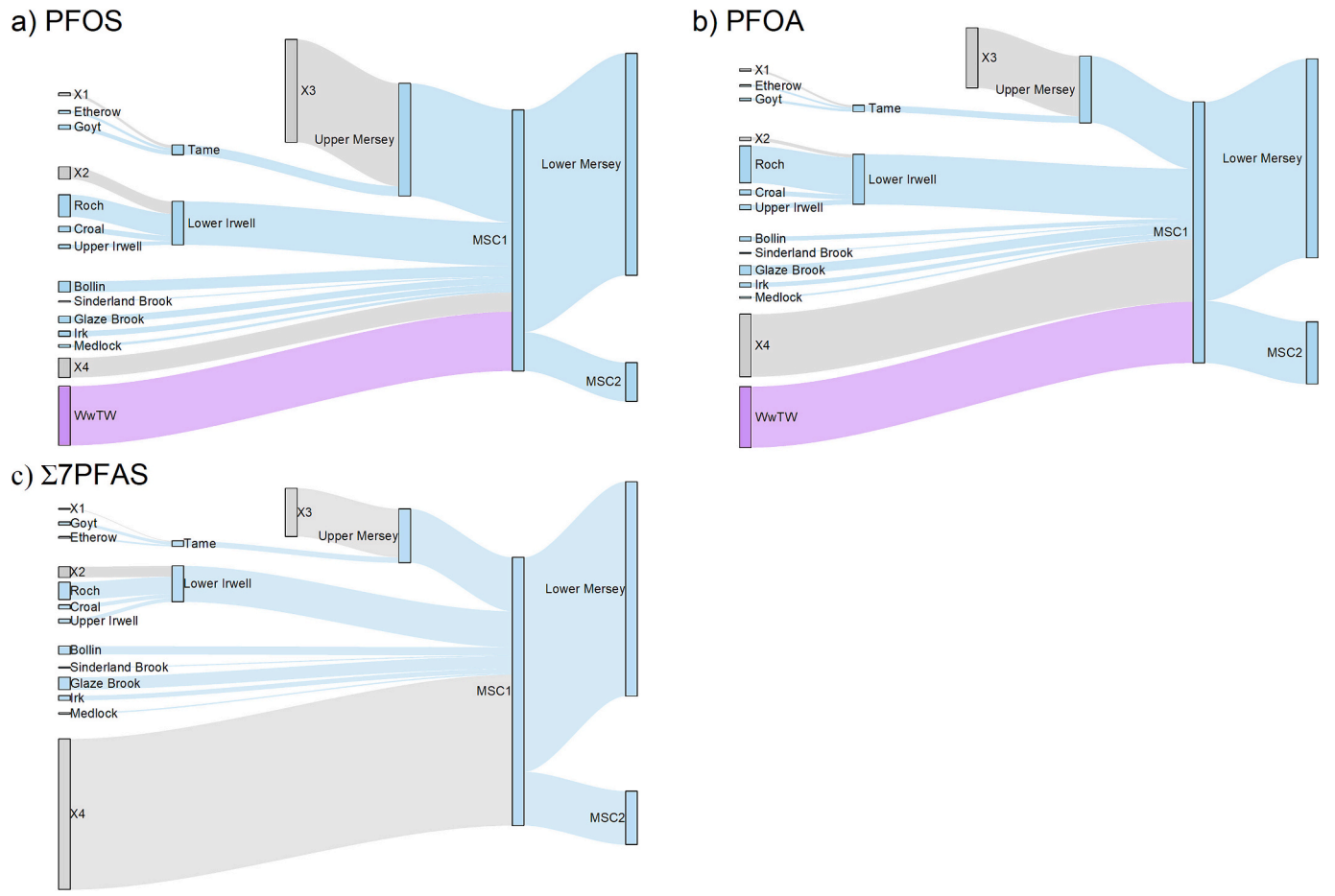

Fig. 5. Sankey diagrams illustrating the change in PFAS loads through the Mersey catchment for PFOS (a), PFOA (b) and the sum of seven PFAS (PFOS, PFOA, PFBS, PFHxA, PFHxS, 6:2FTS, PFHpA) (c). The line thickness is linearly proportional to the load magnitude. The blue lines represent observed loads. The grey lines highlight the location and magnitude of unaccounted for loads in the catchment. The purple lines represent observed loads from WwTW (2015 to 2017 from the UK Chemical Investigation Programme) discharging to the MSC. In this catchment, all of the major tributary rivers flow into the Manchester Ship Canal (MSC1). Further downstream, water in MSC1 overflows into the Lower Mersey and also continues downstream in the canal as MSC2.

3.3. Use of Gd anomalies to discriminate WwTW (population-derived) and Non-WwTW (industry-derived) PFAS Sources

Urban rivers that receive effluents from WwTWs have unique REE patterns displaying positive Gd anomalies due to the use of gadopentetic acid as a contrasting agent in MRI scans (Verplanck et al., 2005). Here, we correlate Gd anomalies with PFAS water concentrations to identify sample sites where WwTW effluents are a probable source and where no large WwTW source is evident. Our analysis of REE concentrations in River Mersey waters designates samples where the percent Gd of the total REE concentration (Gd%) exceeds 15 % as clearly impacted by WwTW. We found approximately 62 % (n = 37) of water samples to have minor or no Gd anomalies (no WwTW source likely) and 38 % (n = 23) of samples to have a Gd anomaly (WwTW source likely) (Figs. S6 and S7). In Fig. 8a-d, PFAS concentration data are plotted against Gd% - the dashed line represents the Gd anomaly threshold of 15 %. Several sample sites plot below the Gd anomaly threshold but have elevated PFAS concentrations. These samples are highlighted in Fig. 8 and correspond to the River Roch (I32-H10, I9-H1, I11-H2) and Glaze Brook (GB1-H20) sites that have high PFHxA, PFHpA, PFOA and PFBS catchment yields. Together, the PFAS loading and Gd anomaly analyses indicate these catchments are substantial sources of non-WwTW (industry) derived PFAS.

The spatial pattern in Gd anomalies is illustrated in Fig. 8e. Sample sites with no Gd anomaly (blue diamonds) occur mostly in the upper part of the Mersey and in all seven major sub-catchments. While some small WwTWs do discharge to the river in these areas, they serve small communities which probably do not have medical (MRI) facilities using gadopentetic acid. It is more likely in these areas that the major sources of PFAS are legacy and contemporary discharges from industrial sources – potentially via small WwTWs. Most of the sample sites with positive Gd anomalies cluster toward the centre of the Mersey catchment and downstream of major WwTWs. Sample sites with elevated PFAS and very large Gd anomalies, included GB1-H20, I30-H8 and B1-H22. These sample sites are located downstream of effluent discharges from Glazebury, Tyldesley and Leigh WwTWs (GB1-H20), from Oldham and Royton WwTWs (I30-H8), and from Macclesfield WwTW (B1-H20). However, any sample sites with Gd% > 15 % can be considered contaminated with PFAS from WwTWs and potentially from other non-WwTW sources.

3.4. Implications for source apportionment of PFAS in post-industrial rivers

This study demonstrates how spatial analysis of PFAS river loads, combined with tracers of wastewater treatment works (WwTW) effluents, can identify PFAS source areas and support geographically based source apportionment. Two key findings are highlighted below.

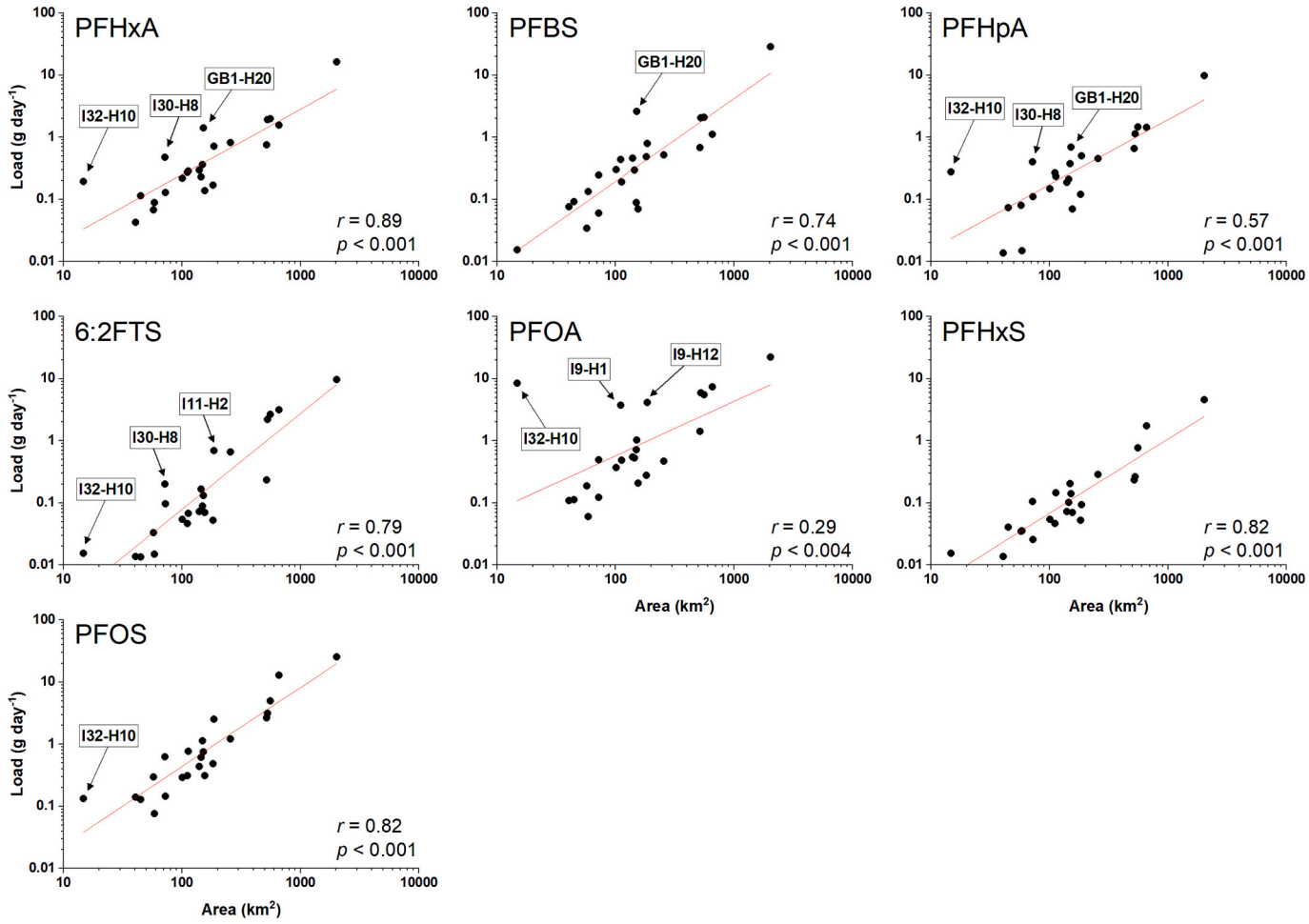

Fig. 6. Scatterplots of PFAS loads against drainage area upstream of the sample point. Note the logarithmic axis scales. *r* and *p* refer to outputs from Pearson's product moment correlation on log-transformed data, where the linear regression model is represented by a red line. Labels are provided for samples sites discussed in the text.

3.5. Spatial analysis of PFAS loads at the catchment-scale identifies geographical source areas

Our analysis of PFAS loads at the outlets of the seven main Mersey sub catchments showed that areas with the highest PFAS concentrations did not always export the highest PFAS loads. For example, PFOS, PFOA, 6:2 FTS and PFHxS loads were greatest from the Upper Mersey (Table 1), despite higher concentrations occurring in northern tributaries. This emphasises the importance of load-based PFAS monitoring, which provides a measure of total mass flux, compared with statistical source apportionment methods that rely only on concentration variability (Kolpin et al., 2021; Silver et al., 2023; Zhang et al., 2016b; Zushi et al., 2011). Without load information, the relative importance of sources cannot be established.

At higher spatial resolution, we mapped PFAS loads along individual river stretches (Fig. 5). This revealed distinct input zones, including the Lower Irwell (Bolton–Manchester), River Tame (Marple Bridge–Stockport), and Upper Mersey (Stockport–Urmston). The largest input occurred to the Manchester Ship Canal (MSC), although these loads were based on historical data. All these reaches, including the MSC, receive inputs from WwTWs, industrial facilities and landfills. Normalising loads by catchment area identified disproportionate yields in certain locations (Fig. 6), notably the River Roch (source–Littleborough) for PFOA, PFHpA and PFHxA, and Glaze Brook for PFBS.

Although we located geographical sources of PFAS inputs, the specific contributions from individual sources remain unknown. This is the logical next step in the river catchment approach, achievable through high resolution synoptic sampling, which has been applied to apportion loads from point and non- point sources in mining impacted rivers. Such approaches are rarely used for PFAS, partly because of the difficulty of acquiring paired flow and water quality data under steady flow conditions in complex, urbanised catchments. Woodward et al. (2024), however, successfully used a time of travel method in a Pennsylvania catchment, isolating PFAS contributions from WwTWs and military bases. Applying similar methods in the Mersey source areas we identified could quantify source contributions and inform targeted remediation. Temporal variability in inputs, driven by hydrology and effluent discharges, adds complexity, but this can be addressed through time variable sampling and modelling (Petre et al., 2022; Byrne et al., 2024).

3.6. Non-WwTW (industrial) PFAS sources are significant in urbanised, post-industrial catchments

WwTWs are well documented PFAS sources to rivers (Coggan et al., 2019; Desgens-Martin et al., 2023), and contribute ~50 % of the PFOS exported from the Mersey (Byrne et al., 2024). However, WwTW inputs alone cannot explain observed PFOS export, implying additional non-WwTW sources and/or in-river transformation of PFAS precursors to PFOS. Precursor degradation in WwTWs, where effluent PFAS loads exceed influents (Moneta et al., 2023; Thompson et al., 2022) supports this possibility. We also observed a large decrease in PFBS load along a stretch of river between the Rivers Goyt and Tame, which may have

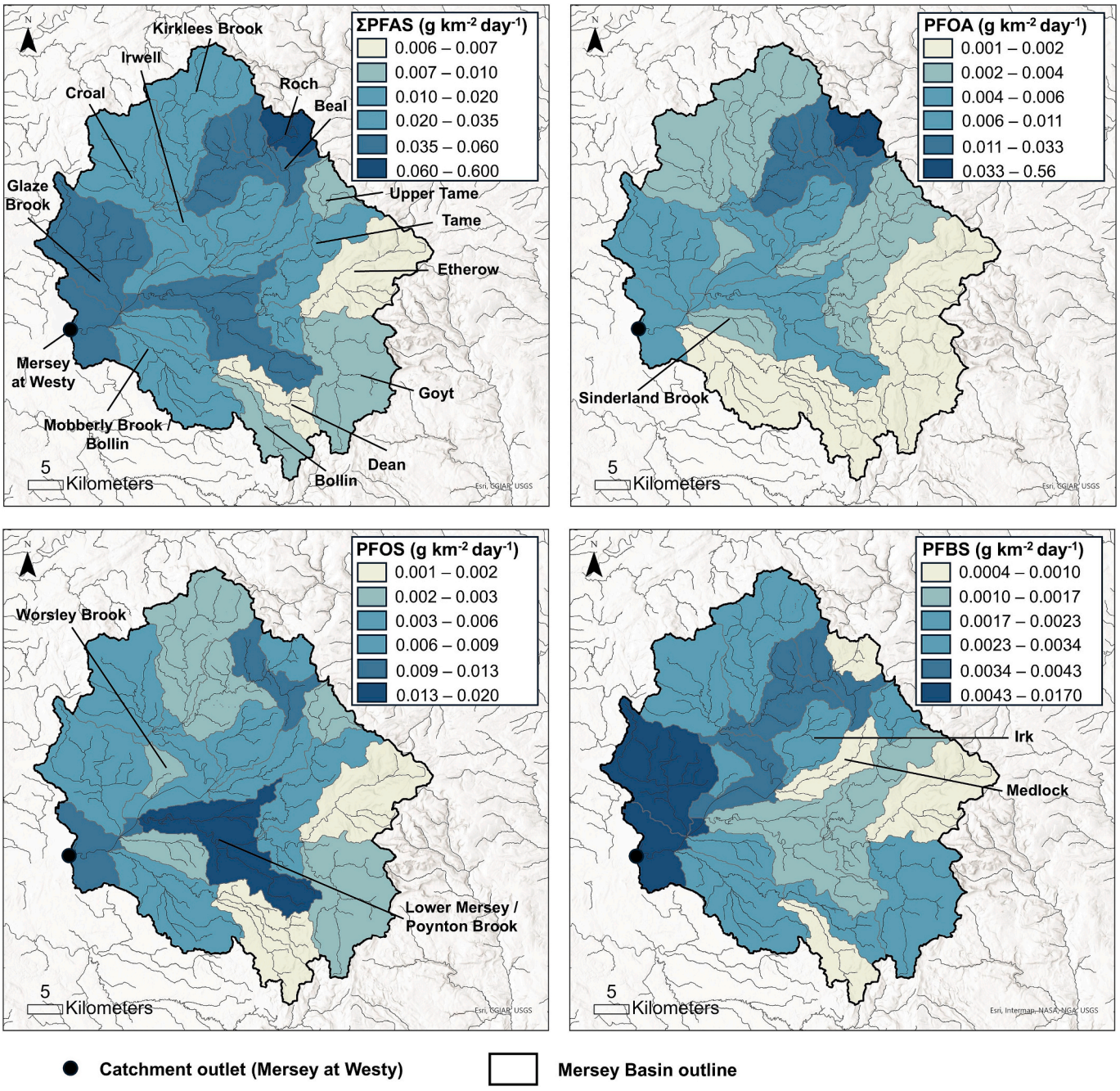

Fig. 7. The River Mersey catchment highlighting selected catchments and associated PFAS yields. The colour ramp is determined by natural breaks in data. Catchment labels are provided for locations referred to in the text.

occurred from sorption to sediments or precursor transformation. Woodward et al. (2024) observed similar behaviours for some PFAS in the Neshaminy Creek, Pennsylvania. We are not aware of any other published studies that have observed this in a river environment. Perhaps this is because a change in concentration alone cannot distinguish losses from dilution or source variability.

Gadolinium (Gd) anomalies, a tracer of WwTW effluent, provided additional insight. Only 38 % of samples displayed Gd anomalies indicative of strong WwTW inputs. The remaining 62 % lacked such signatures, suggesting significant PFAS contributions from non-WwTW sources. These could include industrial discharges and legacy contamination from landfills. The Mersey catchment has no PFAS manufacturing facilities but has a long industrial history, including textiles, paper and printing, tanneries, sawmills, chemical plants, and coal mining. Although heavy industry has declined since the early 20th century, many sites operated into the late 20th century when PFAS use was widespread. This legacy persists through numerous landfills and contaminated land sites. Indeed, headwater catchments such as the River Roch and Glaze Brook exported large PFBS, PFOA, PFHpA and PFHxA yields despite lacking Gd anomalies, consistent with industrial or landfill sources. Gd anomalies have been used previously to trace PFAS from WwTWs in New Mexico, USA (Beisner et al., 2024) but our study is the first to explicitly relate Gd anomalies to PFAS to separate WwTW and non-WwTW sources. This complementary approach enhances spatial loading analysis by providing independent evidence to distinguish industrial and legacy sources from municipal wastewater contributions. While non-targeted analysis (NTA) could provide even greater source resolution, understanding spatial PFAS load patterns remains essential

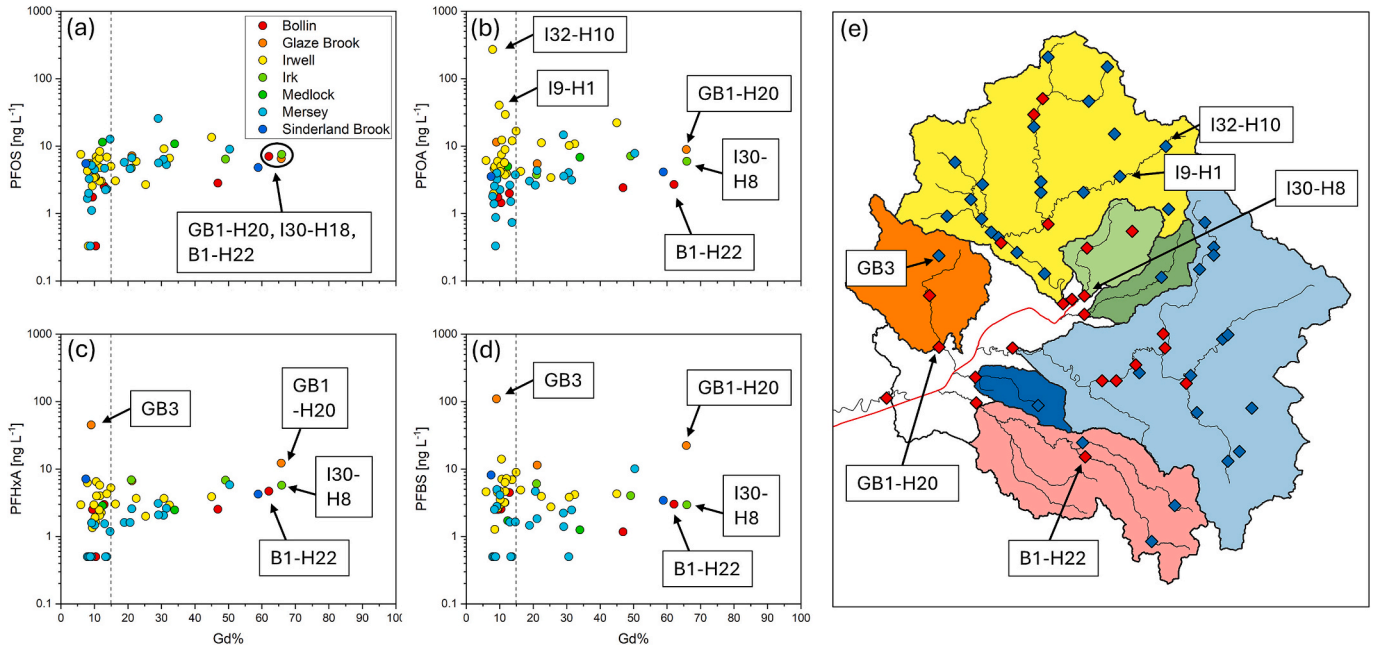

Fig. 8. Scatterplots showing PFAS water concentration against Gd% (a-d). The dashed vertical line represents the Gd anomaly threshold. Catchment labels are provided for sample sites referred to in the text. The Gd data are also plotted on a catchment map (e) where blue diamonds represent samples with no Gd anomaly (Gd% $\leq$ 15 %) and red diamonds represent samples with a positive Gd anomaly (Gd% $>$ 15 %).

to identify and prioritise the areas contributing the largest inputs and posing the highest health and environmental risks.

4. Conclusions

Rivers and their drainage systems play a crucial role in transporting PFAS from terrestrial sources to marine environments, representing a key exposure pathway for ecosystems and humans. In post-industrial river catchments, the multitude of potential PFAS sources complicates efforts to identify priority areas for interventions. This study demonstrates a river catchment-based methodology that integrates synoptic sampling and mass balance analysis to spatially resolve PFAS river loads and isolate key source areas.

In the River Mersey catchment, UK, our analysis reveals that the highest river PFAS concentrations do not necessarily correspond to the highest PFAS loads. This finding highlights a critical risk: interventions based solely on concentration hotspots may overlook areas contributing the largest PFAS loads. Instead, we show that small, headwater sub-catchments – particularly the upper Glaze Brook and River Roch – exhibit the highest PFAS yields (load per unit area). In Glaze Brook, this is likely due to legacy landfill leachates and in the River Roch due to a waste management facility with consented discharge (Fig. 1). Gadolinium anomalies support the widespread influence of WwTWs in controlling river PFAS concentrations, with Gd anomalies evident at 38 % of sample sites where PFAS were also detected. However, our results indicate that industrial sources, especially those emerging post 1950s, may be more significant contributors than previously recognised, with PFAS at 62 % of our sample sites possibly sourced from industry.

Overall, this study provides a scalable monitoring framework for PFAS source apportionment in mixed-source, post-industrial river catchments. We emphasise that while PFAS concentrations inform ecological and human health risk, load-based assessments applied at the river catchment-scale are essential for targeting remediation efforts toward areas delivering the highest mass flux to rivers.

CRediT authorship contribution statement

Patrick Byrne: Writing – review & editing, Writing – original draft, Visualization, Methodology, Investigation, Funding acquisition, Formal analysis, Conceptualization. **William M. Mayes:** Writing – review & editing, Visualization, Methodology, Investigation, Formal analysis, Conceptualization. **Alun L. James:** Writing – review & editing, Methodology, Conceptualization. **Sean Comber:** Writing – review & editing, Formal analysis. **Emma Biles:** Methodology, Investigation, Formal analysis. **Alex L. Riley:** Writing – review & editing, Visualization, Methodology, Investigation, Formal analysis, Conceptualization. **Philip L. Verplanck:** Writing – review & editing, Writing – original draft, Visualization, Methodology, Formal analysis. **Lee Bradley:** Writing – review & editing, Visualization.

Declaration of competing interest

The authors declare that they have no known competing financial interests or personal relationships that could have appeared to influence the work reported in this paper.

Acknowledgements

This research was supported by the Liverpool John Moores University Strategic Research Development Fund. We would like to thank Edie Mayes for her assistance during the field sampling. Any use of trade, firm, or product names is for descriptive purposes only and does not imply endorsement by the U.S. Government. The views expressed in this paper are those of the authors and do not necessarily represent the views of the Environment Agency.

Appendix A. Supplementary data

Supplementary data to this article can be found online at https://doi.org/10.1016/j.scitotenv.2025.180502.

Data availability

Data will be made available on request.

References

Ackerman Grunfeld, D., Gilbert, D., Hou, J., Jones, A.M., Lee, M.J., Kibbey, T.C.G., et al., 2024. Underestimated burden of per- and polyfluoroalkyl substances in global surface waters and groundwaters. Nat. Geosci. 17, 340–346.

Ateia, M., Chiang, D., Cashman, M., Acheson, C., 2023. Total Oxidizable Precursor (TOP) assay—best practices, capabilities and limitations for PFAS site investigation and remediation. Environ. Sci. Technol. Lett. 10, 292–301.

Bau, M., Dulski, P., 1996. Anthropogenic origin of positive gadolinium anomalies in river waters. Earth Planet. Sci. Lett. 143, 245–255.

Beisner, K.R., Travis, R.E., Alvarez, D.A., Barber, L.B., Fleck, J.A., Jasmann, J.R., 2024. Temporal variability and sources of PFAS in the Rio Grande, New Mexico through an arid urban area using multiple tracers and high-frequency sampling. Emerg. Contam. 10, 100314.

Biswas, B., Joseph, A., Parveen, N., Ranjan, V.P., Goel, S., Mandal, J., et al., 2025. Contamination of per- and poly-fluoroalkyl substances in agricultural soils: a review. J. Environ. Manag. 380, 124993.

Breitmeyer, S.E., Williams, A.M., Duris, J.W., Eicholtz, L.W., Shull, D.R., Wertz, T.A., et al., 2023. Per- and polyfluorinated alkyl substances (PFAS) in Pennsylvania surface waters: a statewide assessment, associated sources, and land-use relations. Sci. Total Environ. 888, 164161.

Byrne, P., Onnis, P., Runkel, R.L., Frau, I., Lynch, S.F.L., Edwards, P., 2020. Critical shifts in trace metal transport and remdiation performance under future low river flow scenarios. Environ. Sci. Technol. 54, 15742–15750.

Byrne, P., Mayes, W.M., James, A.L., Comber, S., Biles, E., Riley, A.L., et al., 2024. PFAS river export analysis highlights the urgent need for catchment-scale mass loading data. Environ. Sci. Technol. Lett. 11, 266–272.

Byrne, P., Biles, E., Cui, L., Williams, R., Faustino-Eslava, D.V., Quick, L., et al., 2025. Forever but not everywhere? Unexpected non-detection of per- and polyfluoroalkyl substances (PFAS) in major Philippines rivers. River 4, 29–35.

Cai, Y., Zhang, Q., Ying, G., 2025. Quantifying footprints of perfluorinated compounds in China: from production to discharge into the seas. ACS ES&T Water 5, 920–933.

Calore, F., Guolo, P.P., Wu, J., Xu, Q., Lu, J., Marcomini, A., 2023. Legacy and novel PFASs in wastewater, natural water, and drinking water: Occurrence in Western Countries vs China. Emerg. Contam. 9, 100228.

Charbonnet, J.A., Rodowa, A.E., Joseph, N.T., Guelfo, J.L., Field, J.A., Jones, G.D., et al., 2021. Environmental source tracking of per- and polyfluoroalkyl substances within a forensic context: current and future techniques. Environ. Sci. Technol. 55, 7237–7245.

Coggan, T.L., Moodie, D., Kolobaric, A., Szabo, D., Shimeta, J., Crosbie, N.D., et al., 2019. An investigation into per- and polyfluoroalkyl substances (PFAS) in nineteen Australian wastewater treatment plants (WWTPs). Heliyon 5.

Cookson, E.S., Detwiler, R.L., 2022. Global patterns and temporal trends of perfluoroalkyl substances in municipal wastewater: a meta-analysis. Water Res. 221, 118784.

Cousins, I.T., Johansson, J.H., Salter, M.E., Sha, B., Scheringer, M., 2022. Outside the safe operating space of a new planetary boundary for Per- and Polyfluoroalkyl Substances (PFAS). Environ. Sci. Technol. 56, 11172–11179.

Desgens-Martin, V., Li, W.W., Medina, T., Keller, A.A., 2023. Estimated Influent PFAS loads to wastewater treatment plants and ambient concentrations in downstream waterbodies: case study in Southern and Central California. AXS Es&T Water 3, 2219–2228.

EDINA Digimap Ordnance Survey Service, 2025. OS Open Rivers (SHAPE Geospatial Data), Scale 1:25000, Tiles: GB. In: Ordnance Survey (GB), Editor.

Environment Agency, 2021. Poly- and Perfluoroalkyl Substances (PFAS): Sources, Pathways and Environmental Data, Bristol.

Environment Agency, 2025. Consented Discharges to Controlled Waters with Conditions.

EU. Directive (EU) 2020/2184 of the European Parliament and of the Council of 16 December 2020 on the quality of water intended for human consumption. https://eur-lex.europa.eu/eli/dir/2020/2184/oj.

European Chemicals Agency, 2023. Annex XV Restriction Report - Per- and Polyfluoroalkyl Substances (PFASs).

Evich, M.G., Davis, M.J.B., McCord, J.P., Acrey, B., Awkerman, J.A., Knappe, D.R.U., et al., 2022. Per- and polyfluoroalkyl substances in the environment. Science 375, 512.

Garg, S., Kumar, P., Mishra, V., Guijt, R., Singh, P., Dumee, L.F., et al., 2020. A review on the sources, occurrence and health risks of per-/poly-fluoroalkyl substances (PFAS) arising from the manufacture and disposal of electric and electronic products. J. Water Process. Eng. 38.

Garnett, J., Halsall, C., Thomas, M., Crabeck, O., France, J., Joerss, H., et al., 2021. Investigating the uptake and fate of Poly- and Perfluoroalkylated Substances (PFAS) in sea ice using an experimental sea ice chamber. Environ. Sci. Technol. 55, 9601–9608.

Health Canada, 2023. Per- and Polyfluoroalkyl Substances (PFAS) in Drinking Water.

Ho, S.H., Soh, S.X.H., Wang, M.X., Ong, J., Seah, A., Wong, Y., et al., 2022. Perfluoroalkyl substances and lipid concentrations in the blood: a systematic review of epidemiological studies. Sci. Total Environ. 850.

Joerss, H., Menger, F., Tang, J., Ebinghaus, R., Ahrens, L., 2022. Beyond the tip of the iceberg: suspect screening reveals point source-specific patterns of emerging and novel per- and polyfluoroalkyl substances in German and Chinese Rivers. Environ. Sci. Technol. 56, 5456–5465.

Joseph, N.T., Schwichtenberg, T., Cao, D., Jones, G.D., Rodowa, A.E., Barlaz, M.A., et al., 2023. Target and suspect screening integrated with machine learning to discover per- and polyfluoroalkyl substance source fingerprints. Environ. Sci. Technol. 57, 14351–14362.

Knutsen, H., Mæhlum, T., Haarstad, K., Slinde, G.A., Arp, H.P.H., 2019. Leachate emissions of short- and long-chain per- and polyfluoralkyl substances (PFASs) from various Norwegian landfills. Environ Sci Process Impacts 21, 1970–1979.

Kolpin, D.W., Hubbard, L.E., Cwiertny, D.M., Meppelink, S.M., Thompson, D.A., Gray, J. L., 2021. A Comprehensive Statewide Spatiotemporal Stream Assessment of Per- and Polyfluoroalkyl Substances (PFAS) in an Agricultural Region of the United States. Environ. Sci. Technol. Lett. 8, 981–988.

Kurwadkar, S., Dane, J., Kanel, S.R., Nadagouda, M.N., Cawdrey, R.W., Ambade, B., et al., 2022. Per- and polyfluoroalkyl substances in water and wastewater: a critical review of their global occurrence and distribution. Sci. Total Environ. 809, 151003.

Lawrence, M.G., 2010. Detection of anthropogenic gadolinium in the Brisbane River plume in Moreton Bay, Queensland, Australia. Mar. Pollut. Bull. 60, 1113–1116.

Liu, Z., Liu, J., Zhu, P., Ma, Y., 2024. Interaction and coexistence characteristics of dissolved organic matter and toxic metals with per- and polyfluoroalkyl substances in landfill leachate. Environ. Res. 260, 119680.

Mayes, W.M., Gozzard, E., Potter, H.A.B., Jarvis, A.P., 2008. Quantifying the importance of diffuse minewater pollution in a historically heavily coal mined catchment. Environ. Pollut. 151, 165–175.

Megson, D., Niepsch, D., Spencer, J., Santos, Cd, Florance, H., MacLeod, C.L., et al., 2024. Non-targeted analysis reveals hundreds of per- and polyfluoroalkyl substances (PFAS) in UK freshwater in the vicinity of a fluorochemical plant. Chemosphere 367, 143645.

Moneta, B.G., Feo, M.L., Torre, M., Tratzi, P., Aita, S.E., Montone, C.M., et al., 2023. Occurrence of per- and polyfluorinated alkyl substances in wastewater treatment plants in Northern Italy. Sci. Total Environ. 894, 165089.

National River Flow Archive (NRFA). 2024.

Neill, P., Megson, D., 2024. Landfill leachate treatment process is transforming and releasing banned per- and polyfluoroalkyl substances to UK water. Front. Water 6 - 2024.

Obsekov, V., Kahn, L.G., Trasande, L., 2023. Leveraging systematic reviews to explore disease burden and costs of per- and polyfluoroalkyl substance exposures in the United States. Expo. Health 15, 373–394.

Pelch, K.E., Reade, A., Kwiatkowski, C.F., Merced-Nieves, F.M., Cavalier, H., Schultz, K., et al., 2022. The PFAS-Tox database: a systematic evidence map of health studies on 29 per- and polyfluoroalkyl substances. Environ. Int. 167.

Petre, M.A., Salk, K.R., Stapleton, H.M., Ferguson, P.L., Tait, G., Obenour, D.R., et al., 2022. Per- and polyfluoroalkyl substances (PFAS) in river discharge: Modeling loads upstream and downstream of a PFAS manufacturing plant in the Cape Fear watershed, North Carolina. Sci. Total Environ. 831.

Runkel, R.L., Verplanck, P.L., Walton-Day, K., McCleskey, R.B., Byrne, P., 2023. The truth is in the stream: use of tracer techniques and synoptic sampling to evaluate metal loading and remedial options in a hydrologically complex setting. Sci. Total Environ. 876, 162458.

Ruyle, B.J., Thackray, C.P., Butt, C.M., LeBlanc, D.R., Tokranov, A.K., Vecitis, C.D., et al., 2023. Centurial persistence of forever chemicals at military fire training sites. Environ. Sci. Technol. 57, 8096–8106.

Silver, M., Phelps, W., Masarik, K., Burke, K., Zhang, C., Schwartz, A., et al., 2023. Prevalence and source tracing of PFAS in shallow groundwater used for drinking water in Wisconsin, USA. Environ. Sci. Technol. 57, 17415–17426.

Thompson, K.A., Mortazavian, S., Gonzalez, D.J., Bott, C., Hooper, J., Schaefer, C.E., et al., 2022. Poly- and perfluoroalkyl substances in municipal wastewater treatment plants in the United States: seasonal patterns and meta-analysis of long-term trends and average concentrations. ACS ES&T Water 2, 690–700.

UK Centre for Ecology and Hydrology, 2025. National River Flow Archive, p. 2025.

Verplanck, P.L., Taylor, H.E., Nordstrom, D.K., Barber, L.B., 2005. Aqueous stability of Gadolinium in surface waters receiving sewage treatment plant effluent, Boulder Creek, Colorado. Environ. Sci. Technol. 39, 6923–6929.

Verplanck, P.L., Furlong, E.T., Gray, J.L., Phillips, P.J., Wolf, R.E., Esposito, K., 2010. Evaluating the behavior of gadolinium and other rare earth elements through large metropolitan sewage treatment plants. Environ. Sci. Technol. 44, 3876–3882.

Woodward, E.E., Senior, L.A., Fleck, J.A., Barber, L.B., Hansen, A.M., Duris, J.W., 2024. Using a time-of-travel sampling approach to quantify Per- and Polyfluoroalkyl Substances (PFAS) stream loading and source inputs in a mixed-source, urban catchment. ACS ES&T Water 4, 4356–4367.

Yao, Y., Zhu, H., Li, B., Hu, H., Zhang, T., Yamazaki, E., et al., 2014. Distribution and primary source analysis of per- and poly-fluoroalkyl substances with different chain lengths in surface and groundwater in two cities, North China. Ecotoxicol. Environ. Saf. 108, 318–328.

Zhang, X., Lohmann, R., Dassuncao, C., Hu, X.C., Weber, A.K., Vecitis, C.D., et al., 2016a. Source attribution of Poly- and Perfluoroalkyl Substances (PFASs) in surface waters from Rhode Island and the New York Metropolitan Area. Environ. Sci. Technol. Lett. 3, 316–321.

Zhang, X.M., Lohmann, R., Dassuncao, C., Hu, X.D.C., Weber, A.K., Vecitis, C.D., et al., 2016b. Source attribution of poly- and perfluoroalkyl substances (PFASs) in surface waters from Rhode Island and the New York metropolitan area. Environ. Sci. Technol. Lett. 3, 316–321.

Zhang, M., Zhao, X., Zhao, D., Soong, T.-Y., Tian, S., 2023. Poly- and perfluoroalkyl substances (PFAS) in landfills: occurrence, transformation and treatment. Waste Manag. 155, 162–178.

Zushi, Y., Ye, F., Motegi, M., Nojiri, K., Hosono, S., Suzuki, T., et al., 2011. Spatially Detailed Survey on Pollution by Multiple Perfluorinated Compounds in the Tokyo Bay Basin of Japan. Environ. Sci. Technol. 45, 2887–2893.